MORPHOLOGICAL ANALYSIS OF ALUMINA AND ITS TRIHYDRATE

H. P. Hsieh

Alcoa Laboratories
Aluminum Company of America
Alcoa Center, Pennsylvania 15069
USA

Available morphological analyses for fine particles are briefly reviewed. Three methods for characterizing morphology of alumina and hydrate are studied in some detail: shape factor by Optomax Image Analyzer, signature by sieve cascadography and Fourier method. The shape factor represents only a global deviation from a circle and does not fully reflect small scale protuberances on the particle profile. The sieve cascadography, when fully developed, can be a useful tool for shape characterization. The commercially implemented Fourier analysis provides information on both global and local shape features by its morphological descriptors which can be used for distinguishing various types of particles. An example is given in which a newly defined "blockiness index" from a combination of Fourier descriptors is used to identify and quantify the blocky alumina or hydrate crystals.

Introduction

Particle morphological analysis deals primarily with shape analysis of fine particles. In contrast to size analysis which has been well developed, morphological analysis has started to progress at an accelerating pace only in the last decade. A cross section of various attempts to establish a systematic methodology for shape analysis is given in Figure 1 (1).

Not included in the figure are some new developments such as the sieve cascadography (2,3) and the fractal analysis (4,5). The sieve cascadography will be discussed in some detail in this paper. The fractal analysis was formulated by Mandelbrot (6) for dealing with many naturally occurring boundaries whose profiles have no tangents or differentiable describing functions at many points and cannot be precisely described by the traditional Euclidean geometry and calculus. The underlying notion of the analysis is that dimension is not an absolute quantity but an operational concept. The methodology has been recently applied to the characterization of fine particles (4,5), particularly those possessing rugged boundaries. A quantity called the fractal dimension which has a value between 1 and 2 for a fractal or rugged curve is used to describe the ruggedness of a fine particle profile. The gross shape of the particle, however, is not accounted for. Depending on the nature of the material, a fine particle profile may exhibit different fractal dimensions at different levels of resolution under which the profile is examined.

Most characterization methods are based on two-dimensional images of individual particles as the images are most receptive to the human perception of shape. Other methods, however, infer shape features from physical measurements without information on individual particles. The information content and the uniqueness and completeness of the shape descriptors derived from those schemes also vary. For example, the frequently used ratio of the Martin-to-Feret diameter, the Heywood flatness ratio and elongation ratio contain only four points on a particle profile as the shape information. In contrast, the shape factor, which is defined as 4π (area)/(perimeter)^2, and the Fourier method in principle utilize all the points on the profile.

Many methods use a single parameter to characterize the complex shape features of a particle or an assembly of particles. It is conceivable then that two or more inherently different shapes could have the same value of the parameter, thus creating the problem of nonuniqueness. A few methods circumvent this situation by providing an array of descriptors to distinguish a particle or a sample of particles from others. The Fourier method and the sieve cascadography to be discussed in this paper are examples of such methods.

Three methods for particle shape characterization have been studied and evaluated to some extent: the shape factor, the sieve cascadography and the Fourier analysis. The objective of this paper is to review the feasibility of the three methods for extracting shape information from alumina and hydrate particles.

Shape Factor

As our first attempt at characterizing particle shape, the Optomax Semiautomatic Image Analyzer (by Optomax Inc.) was used for its portion of the system on shape factor determination.

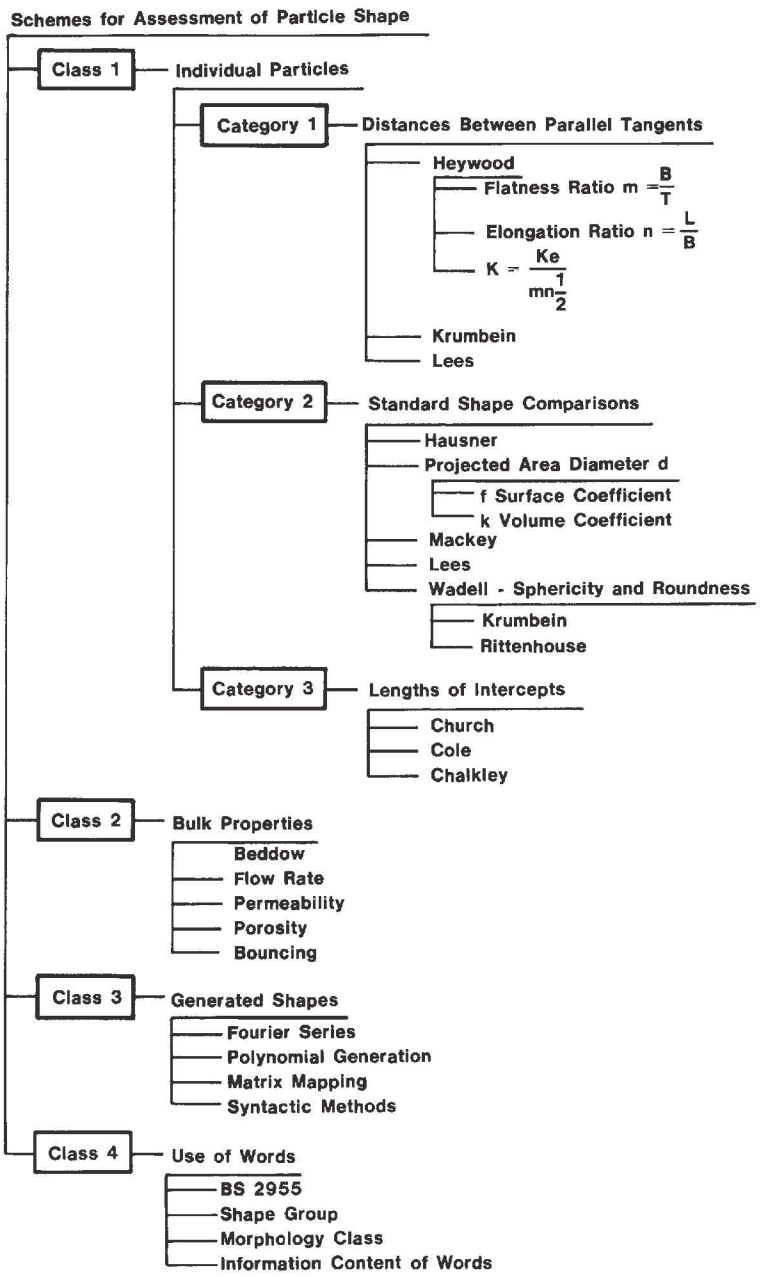

Figure 1. A proposed classification of schemes of shape analysis (after J. K. Beddow)[1]

The system comprises a microcomputer, a TV monitor, a twin floppy disk unit, a graphics tablet, a printer and the image analysis software package. In addition, the video display package includes a TV camera, a camera driver and mixer unit, a microscope interface and support system. With this configuration, either microscopic image or photographic image (e.g., from SEM) can be processed and analyzed. The image appears on the TV monitor. A cursor operated from the graphics tablet stylus appears coincidentally with the image of particles and is used to guide tracing around particles of interest. Tracing is performed using the stylus on the graphics tablet. The image analysis program performs the data and statistical analysis for various geometric features, one of which is the shape factor, σ, which is defined as:

$$\sigma = 4\pi\,(\text{area})/(\text{perimeter})^2 \qquad (1)$$

It is noted that the shape factor is dimensionless and rotationally invariant, i.e., independent of the direction at which the measurement is made.

The shape factor as defined in Equation 1 indicates the degree of departure from being a perfect circle. In the limiting case of a circle, the shape factor becomes 1. For reference purposes, the shape factors for various geometries are given in Table I. It is obvious that the shape factor is small for elongated figure and decreases as the aspect ratio increases. Variation of the shape factor appears to be relatively small for particles or geometries not too different from a circle or square in gross shape. A typical histogram of the shape factor can be seen in Figure 2.

Table I. Shape Factors For Various Geometries

Geometry	Shape Factor*
Circle	1.00
Equilateral Triangle	0.605
Square	0.785
Pentagon	0.865
Hexagon	0.907
Heptagon	0.932
Octagon	0.948
Nonagon	0.959
Decagon	0.967
Rectangle with AR+ = 1.5	0.754
Rectangle with AR = 2.0	0.698
Rectangle with AR = 3.0	0.589
Rectangle with AR = 5.0	0.436
Rectangle with AR = 10.0	0.260

*Shape Factor = $4\pi\,(\text{area})/(\text{perimeter})^2$

+AR = Aspect Ratio = Long side/short side

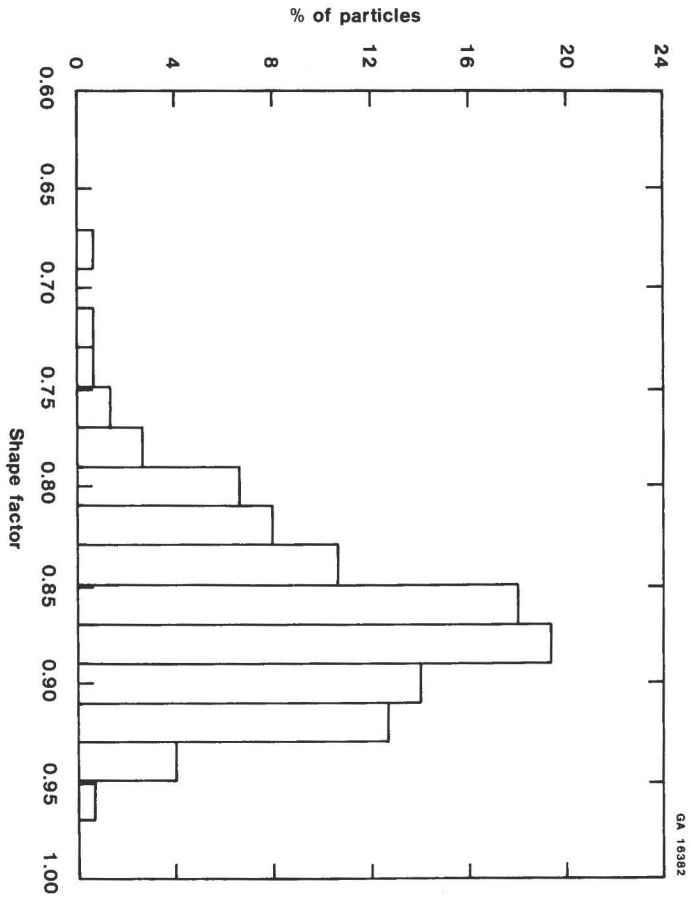

Figure 2. Frequency distribution of shape factor for a hydrate

In an attempt to determine if different size fractions within the same sample show different shape factors, a smelting grade alumina was sieved to the following narrow size fractions: 38-44, 44-61, 61-125, 125-177 and 177-350 μm. The measured shape factors are given in Table II which reveals that the shape factor is about the same within the range of 38 to 177 μm while the coarse fraction shows a smaller value. It appears that to characterize the shape of particles by the shape factor independent of the size effect, samples could be prepared to be within that size range.

Table II. Shape Factors for Various Size Fractions of an Alumina

Sample, μm	Shape Factor	
	Mean	Standard Deviation
38-44	0.839	0.0531
44-61	0.836	0.0560
61-125	0.826	0.0543
125-177	0.836	0.0602
177-350	0.776	0.0651

A wide variety of alumina and hydrate samples were characterized with the shape factor. They represent many sources, both within and outside Alcoa, and different shapes. The mean of the measured shape factor varies from about 0.75 to 0.92. The alumina sample with a mean shape factor of 0.92 is rather spherical while the sample with a value of 0.75 appears very irregular in shape as seen under a light microscope or from SEM photographs.

The shape factor is a lumped parameter for reflecting the global shape features. Like many other single-parameter shape characterizing methods, it suffers from the drawback of low discriminating power among various shapes. For example, the shape factors for the blocky crystals in Figures 3 to 5 are not apparently different from those for aggregates or agglomerates. Thus more sophisticated shape characterization schemes are desirable or necessary for some special applications.

Sieve Cascadography

Unlike the methods based on images such as the shape factor and the Fourier analysis, the concept of sieve cascadography is based on the notion that, for particles with a given size, each particle shape has a characteristic residence time through a cascade of sieves which are identical in opening size and construction and are subject to controlled vibration. Grossly regular and round particles pass through the test system more rapidly than irregular and elongated particles. Thus, measurement of the particle flux exiting the stack of sieves gives the unique shape information or signature of a powder. The presence of a large fraction of particles of a specific shape will be indicated by a peak in the plot representing the residence time of those particles in the sieve stack. The sieve cascadography derives its name from the analogy to the gas or liquid chromatography in that cascading the particles through a number of identical sieves provides temporal separation of particle species (2).

(a). Blocky crystal: Shape factor = 0.841
Blockiness index = 8.12

(b). Aggregate: Shape factor = 0.769
Blockiness index = 0.695

(c). Agglomerate: Shape factor = 0.758
Blockiness index = 0.246

Figure 3. Blockiness index for blocky crystal, aggregate and agglomerate of hydrate

(a). Blocky crystal: Shape factor = 0.843
Blockiness index = 11.2

(b). Aggregate: Shape factor = 0.744
Blockiness index = 0.480

(c). Agglomerate: Shape factor = 0.807
Blockiness index = 0.346

Figure 4. Blockiness index for blocky crystal, aggregate and agglomerate of cooler discharge alumina

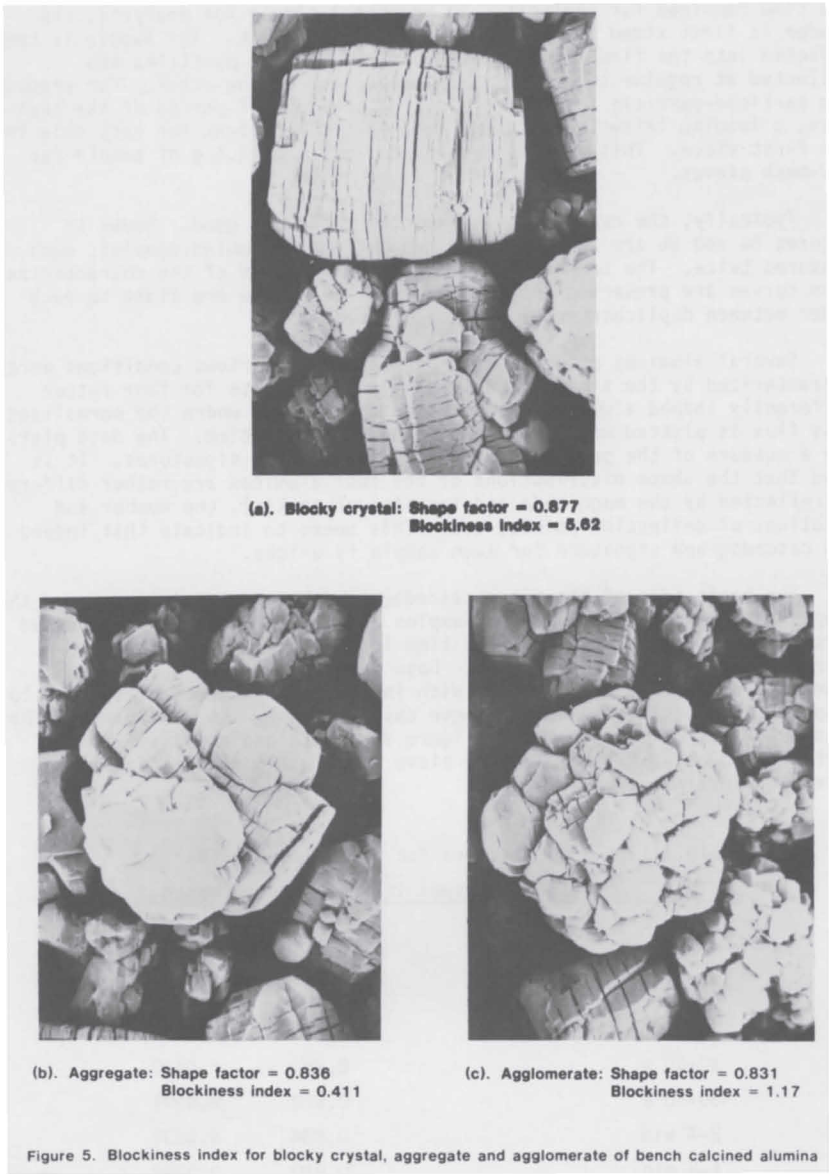

(a). Blocky crystal: Shape factor = 0.877
Blockiness index = 5.62

(b). Aggregate: Shape factor = 0.836
Blockiness index = 0.411

(c). Agglomerate: Shape factor = 0.831
Blockiness index = 1.17

Figure 5. Blockiness index for blocky crystal, aggregate and agglomerate of bench calcined alumina

It has been established that for a good and practical gross separation, -100+120 mesh or comparable fractions of powders could be used to pass through a stack of 20 identical 100-mesh sieves (3). It is noted that increasing the number of sieves used increases both the resolution and the time required for analysis. To prepare a sample for analysis, the powder is first sized for 10 minutes on a sieve stack. The sample is then injected into the first (top) sieve at start and the particles are collected at regular time intervals at the base of the stack. For preventing particle-particle interference during the initial period of the analysis, a loading criterion is used: one particle or less for each hole in the first sieve. This usually amounts to less than 2.5 g of sample for 100-mesh sieves.

Typically, the reproducibility of the method is good. Shown in Figures 6a and 6b are test data for two different alumina samples, each measured twice. The trends and the deflection points of the characterization curves are preserved and, in general, the curves are close to each other between duplicate runs.

Several aluminas produced or processed under various conditions were characterized by the sieve cascadography. The results for four rather differently shaped aluminas are compared in Figure 7 where the normalized mass flux is plotted as a function of the residence time. The data plots are a measure of the powders' shape distributions or signatures. It is seen that the shape distributions of the four aluminas are rather different as reflected by the magnitude and location of peak(s), the number and locations of deflection points, etc. This seems to indicate that indeed the cascadograph signature for each sample is unique.

The basic idea of the sieve cascadography has been examined using the shape factor described earlier. Samples of a given alumina which passed through the sieve stack at various time intervals were collected and characterized by the shape factor. Data in Table III which shows a generally decreasing shape factor with increasing residence time seems to support the practicality of the sieve cascadography. As confirmed by the scanning electron micrographs in Figure 8, smooth and relatively round particles move rapidly through the sieve stack while more elongated or irregular particles move slowly.

Table III. Shape Factors for Particles with Various Residence Times in Sieve Cascadograph

Sample Residence Time	Shape Factor Mean	Shape Factor Standard Deviation
Starting Material	0.866	0.0670
10-20 s	0.895	0.0400
30-60 s	0.872	0.0501
2-4 min	0.834	0.0676
4-8 min	0.830	0.0792
8-16 min	0.833	0.0682
32-64 min	0.829	0.0788

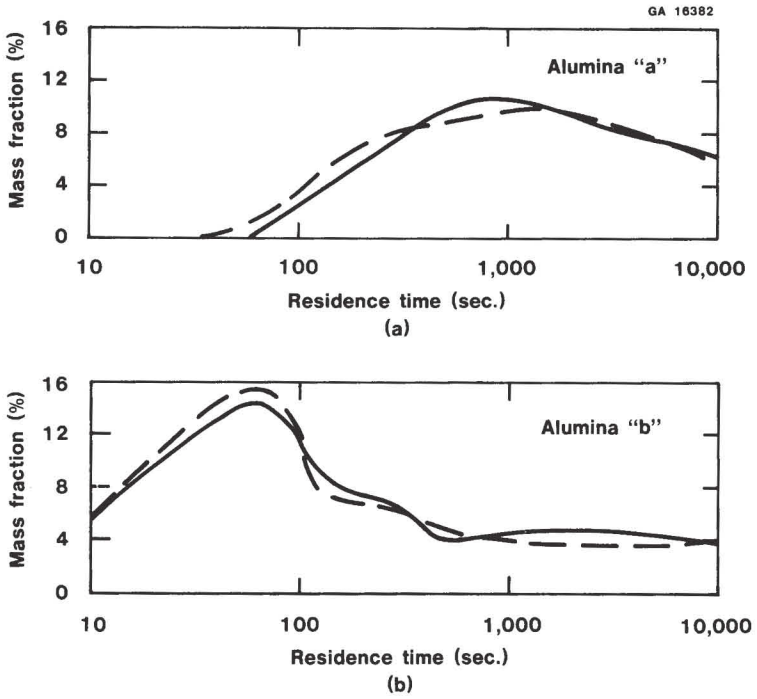

Figure 6. Reproducibility tests for sieve cascadography

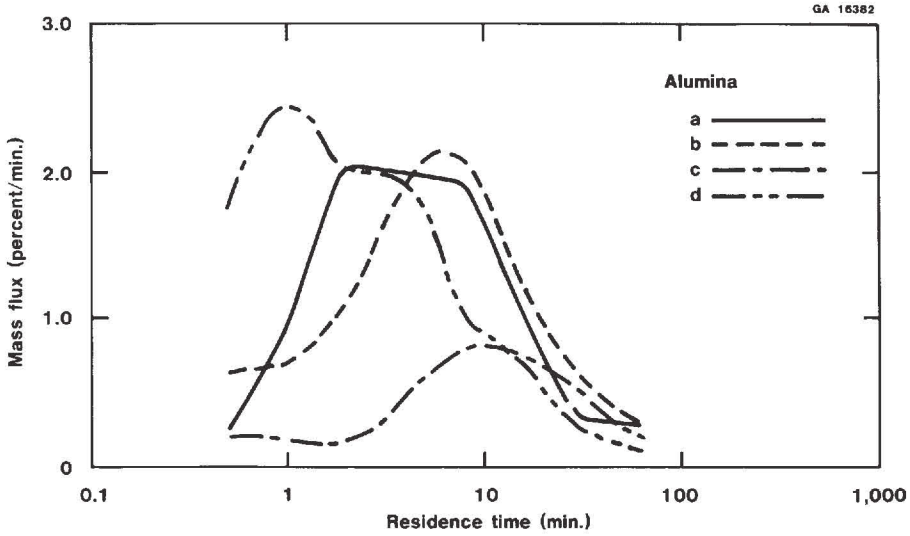

Figure 7. Characterization curves of various aluminas by sieve cascadography

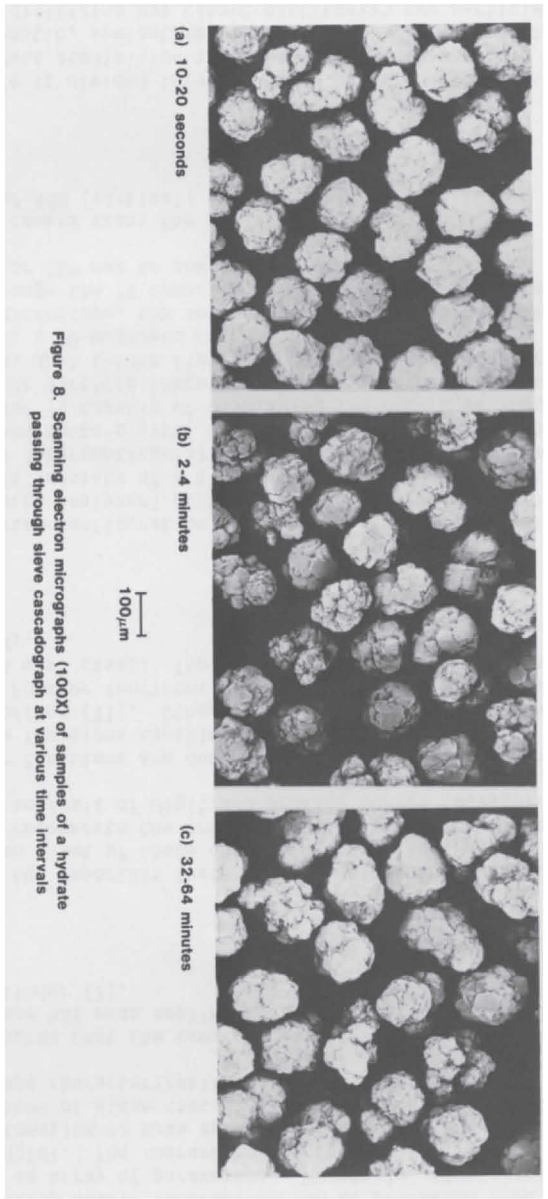

Figure 8. Scanning electron micrographs (100X) of samples of a hydrate passing through sieve cascadograph at various time intervals

The signature curves obtained from the sieve cascadography are currently difficult to interpret and, in some cases, experience is required to use the signature for distinguishing samples with subtle differences. From the practical point of view, it would be desirable in further developments if readily usable information can be extracted from the data plots in the form of an array of parameters. Hopefully, these parameters are physically meaningful. The improvement in data analysis, coupled with refinement and automation in data acquisition hardware and techniques, should make the method of sieve cascadography an operationally simple and useful tool for shape characterization and classification.

It is noted that the same concept of residence time as a function of particle shape has been applied to a similar technique using a tilted, rotating cylinder (7).

Fourier Analysis

One of the important features of a unique and adequate shape analysis is that given a set of shape descriptors derived from the analysis one can technically regenerate the original particle profile. One such method is the Fourier analysis of digitized profile points (8,9,10).

Fourier functions are one of several sets of orthogonal, normalized and complete functions capable of adequately representing the complicated particle profiles (11). Other functions include Walsh functions and Haar functions. Fourier functions, however, are more widely used and rather effective in most cases. The method of Fourier analysis has been examined in this study.

Hardware

The system configuration used for the Fourier analysis of particle profiles (Shape Analyzer™ by Shape Technology) is schematically shown in Figure 9. It consists of a high quality TV camera connected to a microcomputer (by Intercontinental Micro Systems with a Z-80A microprocessor) through an analog-to-digital converter with an accompanying TV monitor. The TV monitor is capable of displaying the real time image as well as "freezing" the particle images for analysis in the computer. The system also contains dual 8-inch floppy disk drives, a 70-megabyte hard disk for mass storage, a 20-megabyte streaming tape for backup and a printer. With an optical microscope, the morphology of a fine particle may be studied directly through the TV camera. Alternatively, a photographic image such as from SEM or TEM may be analyzed.

The TV camera scans the field of view horizontally. The field has a resolution of 480 (vertical) X 512 (horizontal) pixels or cells.

Software

Software is divided into two major parts: data acquisition and data analysis. Data acquisition involves digitizing images in three different modes: automatic, semiautomatic and manual. The automatic mode provides the fastest digitizing but cannot distinguish two particles in contact with each other from a single integral particle. If the particles are well dispersed, this mode of digitizing can be used with ease and speed. The semiautomatic mode permits the choice of whether a specific particle should

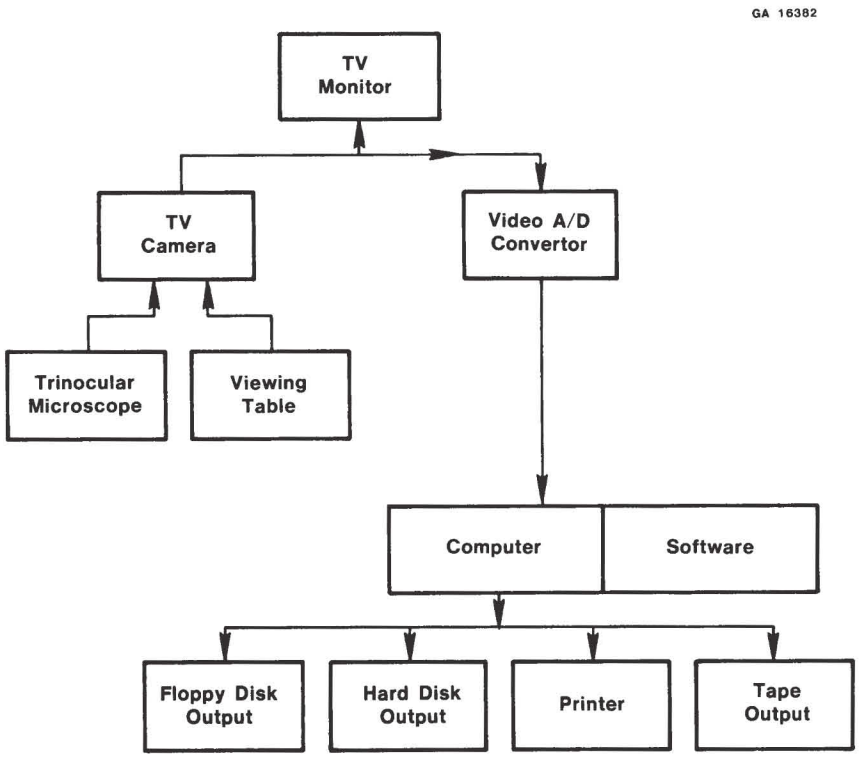

Figure 9. Automated image analyzing system, Shape Analyzer (TM)

be considered and does this automatically from particle to particle within the same window frame on the screen. This mode is generally preferred. The manual mode is used with a keyboard-controlled cursor to move to the desired particle for image digitization. In any mode, particles which only partially appear within the window frame are automatically excluded for analysis. Data analysis is performed by the Fourier method with final results in the form of a set of morphological descriptors. These descriptors have unique physical meanings.

Profile Tracing

The particle profiles are first observed by the TV camera. At the operator's response for accepting the image, the analog video signals are sent to the analog-to-digital converter where the analog signals are converted to digital signals which are then transferred to the computer.

Based on the concept of "contour following" (12), the image digitizing, or specifically edge tracing, is done by comparing the video data with a preset threshold gray level. This threshold number is the estimate of the gray level that best differentiates between the image and the background. The gray level 0 is the darkest and level 255 the brightest. Consider the case of dark images in light background. Points with gray levels lower (that is, darker) than the threshold number are considered to be within the image; those with higher gray levels are considered as background. Based on this procedure, the edges of the particle image may be traced. The program has been written to show the traced profile (or extracted edge) immediately superimposing the particle image that has been digitized. Thus, the operator can examine whether a threshold value has been properly selected within a range.

There are two major factors which will cause the digitized (x, y) points to deviate from "true" edge points. First, due to the fact that the (x, y) data obtained from the digitizing process are discrete in nature, roundoff error is involved. Second, some degree of fuzziness of the edges can exist due to the variation in gray levels. As a consequence of these factors, certain amounts of high frequency noise are present in the image of the particle profile. The noise is filtered by means of a statistical procedure (13). The "smoothed" digitized points are then checked for possible reentrant portions before data are analyzed by the R-θ Fourier method to be discussed later.

Fourier Method

Three major Fourier methods have been developed: the R-θ method (8, 14), the ϕ-ℓ method (15) and the R-S method (16). All methods utilize the Fourier transform on the points of the particle profile to obtain their own morphological descriptors. In the R-θ method, the (x, y) pairs or coordinates are converted to polar coordinates or (R, θ) pairs, using the center of gravity of the particle image as the origin (Figure 10). These (R, θ) pairs are then expanded into a Fourier series and the descriptors are calculated from the Fourier coefficients. In the ϕ-ℓ method, the (x, y) pairs are transformed to (ϕ, ℓ) pairs where ϕ and ℓ represent the angular direction of the particle profile and the arc length, respectively (Figure 11). Similarly, the function $\phi(\ell)$ is then normalized and expanded into a Fourier series the coefficients of which are used for obtaining the descriptors. Finally, in the R-S method, the (x, y) coordinates of the profile are first transformed into a polar representation of (R, θ). A

GA 16382

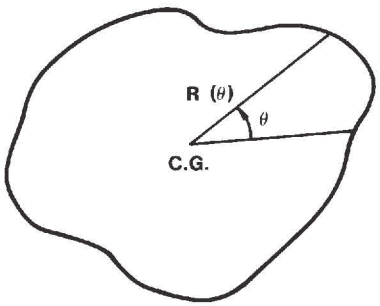

Figure 10. Schematic of R-θ Fourier method

GA 16382

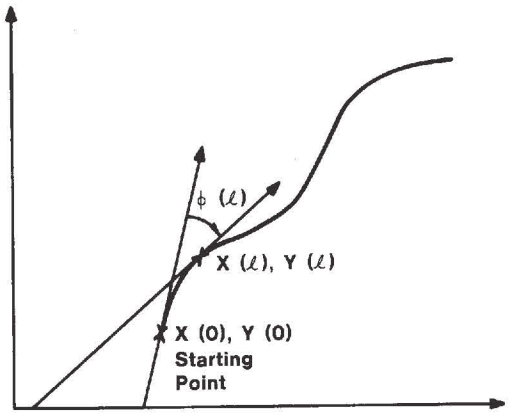

Figure 11. Schematic of ϕ-ℓ Fourier method

Fourier series expansion is used to express R as a function of the normalized arc length, S. Another Fourier series is used to represent $d\theta/dS$ as a function of S also. The Fourier coefficients for both expansions, R(S) and $d\theta/dS$, can then be used to generate morphological descriptors.

The R-θ method has the advantage of storing all the size and shape information analytically in the descriptors. It, however, cannot handle particles with an appreciable number of reentrant points (Figure 12). From our past experiences, alumina and hydrate particles do not exhibit the reentrant problems. In contrast, the ϕ-ℓ method can analyze more complex shapes. But it suffers from the disadvantage that important quantities in physical applications such as the area, moment of inertia, etc, cannot be found analytically and must be found using numerical integration techniques. It also does not yield size information as in the R-θ method. Like the ϕ-ℓ method, the R-S method is not affected by reentrant points on the particle profile. It is possible to calculate quantities such as the area, moment of inertia, etc, analytically. Due to its need to calculate two Fourier series, the R-S method is slower. The R-θ method and the R-S method are statistically similar but geometrically different.

The particular Fourier method used in this study is the R-θ method due to its simplicity and ease of interpretation. But the other methods can be implemented in the analysis without much difficulty.

Beddow (8) has shown that many two-dimensional particle profiles, such as those from digitization described earlier, may be reproduced quite well if the boundary of a profile is expanded as a truncated Fourier series of the polar coordinates (R, θ) using the center of gravity as the origin:

$$R(\theta) = a_o + \sum_{n=1}^{N} (a_n \cos n\theta + b_n \sin n\theta) \qquad (2)$$

where a_o, a_n and b_n are the Fourier coefficients and contain all of the size and shape information and n is the harmonic number. It is noted that the above Fourier coefficients are determined by a fast Fourier transform method. The above representation for a particle shape, however, is not unique in that the Fourier coefficients in Equation 2 are rotationally variant. This means that the same shape, in different orientations, will not have the same set of Fourier coefficients. It is necessary that adequate size and shape descriptors be developed.

The following terms can be shown to be size invariant and rotationally invariant (14):

$$R_o = \sqrt{a_o^2 + \frac{1}{2} \sum_{n=1}^{\infty} (a_n^2 + b_n^2)} \qquad (3)$$

$$L_o = \frac{a_o}{R_o} \qquad (4)$$

GA 16382

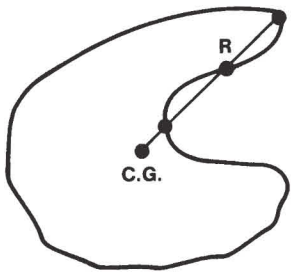

Figure 12. Particle with re-entrant points

$$L_1(n) = 0 \text{ for all } n \tag{5}$$

$$L_2(n) = \frac{1}{2R_o^2}\left(a_n^2 + b_n^2\right) \quad (n=1, 2, 3...N) \tag{6}$$

$$L_3(m,n) = \frac{3}{4R_o^3}\left(a_m a_n a_{n+m} - b_m b_n a_{n+m} + a_m b_n b_{n+m} + b_m a_n b_{n+m}\right) \quad (n+m = 2, 3, 4...N) \tag{7}$$

where a_o is the mean radius with respect to the polar angle, θ.

Many of the above morphological descriptors are physically significant. For example, the "equivalent radius," R_o, is the radius of a circle having the same area as that of the particle profile. The term L_o is the size normalized mean radius of the particle profile with respect to θ. The shape term $L_2(2)$ reflects elipticity or elongation of the particle profile. It is related to the classical shape feature "aspect ratio" of a particle profile. That is, $L_2(2)$ is generally larger for an elongated particle. It is usually based on a measurement of many points on the profile as opposed to the classical method which employs only a few points. $L_2(3)$ represents the closeness of a particle profile to be an equilateral triangle. Likewise, $L_2(4)$, $L_2(5)$ and $L_2(6)$ indicate the degree to which a particle profile resembles a four-sided or "blocky," five-sided and six-sided geometric figure, particularly if it is not far from being an equilateral polygon. Thus, $L_2(3)$ term dominates the series for a triangle and $L_2(4)$ term is orders of magnitude greater than other $L_2(n)$ terms for a square. Likewise, $L_2(5)$ and $L_2(6)$ are the most significant terms for a pentagon and hexagon, respectively. Therefore, the proper $L_2(n)$ term can be used as one of the important shape classifiers with respect to simple overall geometries.

The $L_2(n)$ terms generally become progressionally smaller as n increases. The $L_2(n)$ terms described global shape properties. Two other important terms can be derived from the $L_2(n)$ series:

$$\Omega = \text{Radance} = \sum_{n=1}^{N} L_2(n) \tag{8}$$

and

$$\Psi = \text{Roughness} = \sum_{n=7}^{N} L_2(n) \tag{9}$$

where Ω, the radance or not-roundness, is a measure of the deviation from being a perfect circle and, Ψ, the roughness sums up the protuberances or small-scale perturbations on the particle profile.

As shown in Figure 13, the roughness progressionally increases with increasing protuberances added to a circle. Thus, it appears that the term defined in Equation 9 does indicate the degree of roughness on a particle profile. It is noted that the choice of 7 as the starting term of the series in Equation 9 for the roughness is more or less arbitrary. The reasoning behind the choice of 7 is that any terms of higher order than $L_2(6)$ do not significantly influence the overall or global shape of the particle. Instead they reflect the finer details of the profile. Sometimes it is also useful to employ a quantity called skewness which is defined as:

$$\Phi = \text{Skewness} = \sum_{m=1}^{N} \sum_{n=1}^{N} L_3(m,n) \qquad (10)$$

It is noted that one of the strong points of the Fourier method is that the morphological descriptors given in Equations 3 through 7 can be used to regenerate the original particle profile. Thus, contrary to many other shape analysis with a single or few usable parameters, the Fourier method is unique and complete. And as mentioned earlier, the generated morphological descriptors are size, translationally and rotationally invariant.

Application

The Fourier analysis has been applied to a case where blocky alumina or hydrate particles are objectively identified and quantified among agglomerate or aggregate particles. The massive blocky crystals, if present, have significant impacts on the characteristics of the final alumina products.

Figures 3, 4 and 5 display the massive single prismatic particles compared with aggregates and agglomerates for one hydrate and two calcined aluminas. Two more blocky hydrate crystals are shown in Figures 14a and 14b. Examination of Figures 3 to 5 and 14 reveals that the blocky crystals possess two distinct characteristics that can be easily detected by the shape analysis via the Fourier method. One is that their global or overall shape appears to be four-sided (square or slightly rectangular). Thus, $L_2(4)$ values for those crystals should be large compared with those for aggregates or agglomerates. The other is that their edges are relatively smooth unlike the proturberances or small-scale perturbations typical of aggregates or agglomerates. Therefore, the roughness term, Ψ, given in Equation 9 should be small.

Each particle in Figures 3 to 5 and 14 was digitized and analyzed five times to obtain an average set of values for the various morphological descriptors. Given in Table IV are some of the morphological descriptors. Indeed, $L_2(4)$ and Ψ, the roughness, are the two descriptors that consistently have the power to distinguish blocky crystals from aggregates or agglomerates. In general, the $L_2(4)$ term is much higher and the roughness term is much lower for blocky crystals than for aggregates or agglomerates.

GA 16382

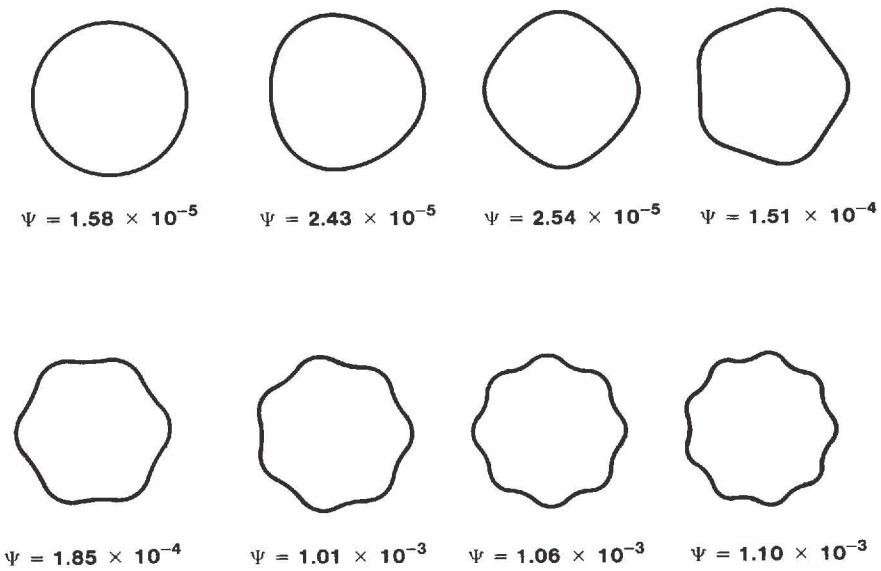

Figure 13. Effect of perturbations to a circle on roughness, Ψ, from Fourier analysis

TABLE IV. Morphology of Blocky Crystals, Aggregates and Agglomerates of Alumina and Hydrate

Particle ID (Figure No.)	3(a)	4(a)	5(a)	14(a)	14(b)	3(b)	4(b)	5(b)	3(c)	4(c)	5(c)
Particle Description	Blocky	Blocky	Blocky	Blocky	Blocky	Aggreg.	Aggreg.	Aggreg.	Agglom.	Agglom.	Agglom.
L_o	9.86E-01	9.94E-01	9.98E-01	9.87E-01	9.98E-01	9.95E-01	9.83E-01	9.95E-01	9.96E-01	9.94E-01	9.96E-01
Radance	2.69E-02	1.15E-02	3.89E-03	2.59E-02	3.81E-03	9.58E-03	3.29E-02	1.07E-02	7.33E-03	1.20E-02	7.98E-03
Roughness	2.52E-04	3.84E-04	4.30E-04	1.25E-04	2.15E-04	1.61E-03	7.70E-04	9.32E-04	1.67E-03	1.25E-03	7.84E-04
Skewness	8.79E-04	1.04E-03	1.01E-04	2.49E-04	1.40E-05	7.73E-05	1.48E-03	2.01E-04	4.04E-04	3.89E-04	1.22E-05
$L_2(2)$	2.36E-02	6.19E-03	2.78E-04	2.36E-02	1.14E-03	2.82E-03	2.73E-02	7.88E-03	1.08E-03	8.64E-03	4.98E-03
$L_2(3)$	2.68E-04	2.94E-04	6.36E-04	1.08E-04	2.64E-04	1.78E-03	5.18E-04	9.97E-04	2.49E-03	1.37E-03	6.09E-04
$L_2(4)$	2.05E-03	4.30E-03	2.42E-03	1.70E-03	2.11E-03	1.12E-03	3.70E-04	3.83E-04	4.09E-04	4.34E-04	9.18E-04
$L_2(5)$	2.94E-05	2.03E-04	1.21E-04	1.55E-05	4.50E-05	2.01E-04	3.49E-03	4.49E-04	1.38E-03	4.57E-05	2.90E-04
$L_2(6)$	6.50E-04	1.41E-04	2.91E-06	3.05E-04	3.51E-05	2.02E-03	4.41E-04	2.03E-05	2.89E-04	2.02E-04	3.96E-04
BI* = $L_2(4)$/ Roughness	8.12E+00	1.12E+01	5.62E+00	1.36E+01	9.88E+00	6.95E-01	4.80E-01	4.11E-01	2.46E-01	3.46E-01	1.17E+00
Note	Hydrate	Alumina	Alumina	Hydrate	Hydrate	Hydrate	Alumina	Alumina	Hydrate	Alumina	Alumina

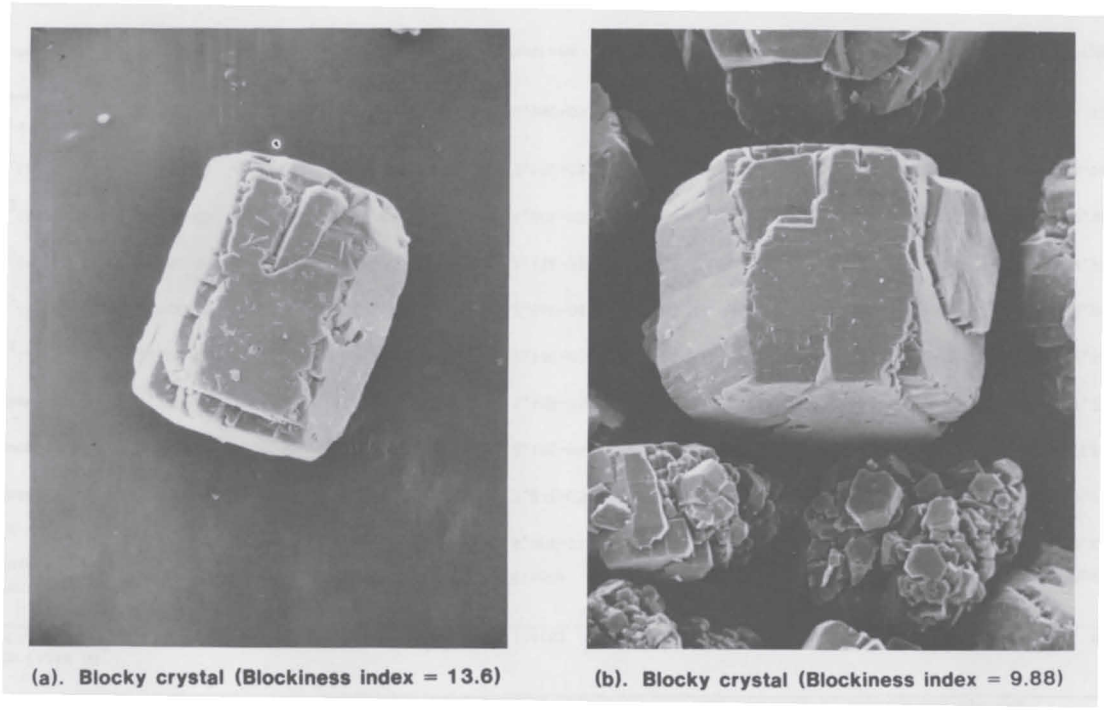

(a). Blocky crystal (Blockiness index = 13.6)

(b). Blocky crystal (Blockiness index = 9.88)

If we combine the above two shape classifiers by defining a new term called "blockiness index" (BI)

$$BI = \frac{L_2(4)}{\Psi}, \qquad (11)$$

the difference between single blocky crystals and agglomerates (or aggregates) would be even more distinct. In fact, as shown in Table IV and in Figures 3 to 5 and 14, the blockiness index for single blocky crystals is generally greater than 5 while for aggregates and agglomerates it is generally much less than 1 although the agglomerate shown in Figure 5 has a BI value of 1.17.

Thus by analyzing the digitized particle images of hydrate or alumina samples through the Fourier analysis, one can assess objectively the percentage of blocky crystals in the population of particles. This can be especially useful when the camera views can be staged automatically to move from field to field within a given sample.

Conclusions

Compared to size analysis which has been well developed, studies of particle morphology and its effects on processing and handling characteristics of powders have started to progress at an accelerating pace only in the last decade. Available morphological analyses for fine particles are briefly reviewed. Three methods for characterizing morphology of alumina and hydrate are studied in detail. The shape factor is a single-parameter approach and represents only a global deviation from a circle. It does not fully reflect small-scale roughness on a particle profile. The sieve cascadography uses the notion that a particle has a residence time characteristic of its shape. The method, when fully developed in data acquisition and analysis, can be a useful tool for shape characterization. The commercially implemented Fourier analysis describes both global and local shape features by its morphological parameters which can be used to distinguish various types of particles. The method is applied to identifying blocky alumina and hydrate crystals among agglomerate and aggregate particles through a newly defined "blockiness index."

Acknowledgments

The sieve cascadography tests were performed by the West Virginia University Particle Analysis Center under the guidance of Professor T. P. Meloy. Messrs. G. J. DiFranco and L. L. Lizik assisted in determinations of the shape factor and the Fourier analysis descriptors.

References

1. J. K. Beddow, Particle Science and Technology, p. 438, Chemical Publishing Co., Inc., New York, N.Y., 1980.

2. T. P. Meloy and K. Makino, "Characterizing Residence Times of Powder Samples on Sieves," Powder Technology, 36 (2) (1983), pp. 253-258.

3. T. P. Meloy, N. Clark, and T. E. Durney, "The Sieve Cascadograph — An Instrument for the Measurement of Particle Shape Distribution," paper presented at the 9th Annual Powder & Bulk Solids Conference, Rosemont, Il., May 15-17, 1984.

4. B. H. Kaye, "Specification of the Ruggedness and/or Texture of a Fine Particle Profile by Its Fractal Dimension," Powder Technology, 21 (1) (1978), pp. 1-16.

5. H. Schwarz and H. E. Exner, "The Implementation of the Concept of Fractal Dimension on a Semi-Automatic Image Analyzer," Powder Technology, 27 (2) (1980), pp. 207-213.

6. B. B. Mandelbrot, Fractals: Form, Chance and Dimension, W. H. Freeman & Co., New York, NY, 1977. (Also, The Fractal Geometry of Nature, revised ed. 1983).

7. M. Furuuchi and K. Gotoh, "Shape Characterization of Granular Materials from the Residence Time in a Tilted, Rotating Cylinder," paper presented at Fine Particles Society Annual Meeting, Orlando, Fl., July 30-August 1, 1984.

8. J. K. Beddow and G. C. Philip, "Fourier Analysis — Synthesis Method of Particle Shape Analysis," Planseeberichte fur Pulvermetallurgie, 23 (1) (1975), pp. 3-14.

9. H. P. Schwarz and K. C. Shane, "Measurement of Particle Shape by Fourier Analysis," Sedimentology, 13 (1969), pp. 213-231.

10. R. Ehrlich and B. Weinberg, "An Exact Method for Characterization of Grain Shape," Journal of Sedimentary Petrology, 40 (1) (1970), pp. 205-212.

11. J. K. Beddow, "Particle Morphological Analysis," pp. 1-84 in Advanced Particulate Morphology, J. K. Beddow and T. P. Meloy, ed.; CRC Press, Inc., Boca Raton, Fl., 1980.

12. R. O. Duda and P. E. Hart, Pattern Classification and Scene Analysis, p. 290, John Wiley and Sons, Inc., New York, N.Y., 1973.

13. C. Chang, "Particle Morphology and Its Effect on Bulk Property," Ph.D. Thesis, University of Iowa (1982).

14. D. W. Luerkens, J. K. Beddow, and A. F. Vetter, "Morphological Fourier Descriptors," Powder Technology, 31 (2) (1982), pp. 209-215.

15. C. T. Zahn and R. Z. Roskies, "Fourier Descriptors for Plane Closed Curved," IEEE Trans. Computers, C21 (3) (1972), pp. 269-281.

16. D. W. Luerkens, J. K. Beddow, and A. F. Vetter, "A Generalized Method of Morphological Analysis (the (R, S) Method)," Powder Technology, 31 (2) (1982), pp. 217-220.